

Ion Transport in Nanocomposites

A. B. Yaroslavl'tsev

*Kurnakov Institute of General and Inorganic Chemistry, Russian Academy of Sciences,
Leninskii pr. 31, Moscow, 119991 Russia
e-mail: yaroslav@igic.ras.ru*

Received January 10, 2009

Abstract—Successive analysis of interface defect formation and its implications for the ionic conductivity was carried out for ionically conducting nanocomposites that hold much significance for technological applications. It was shown that the most efficient way to prepare such composites is through the use of nanosized particles. A review was made of the current state of research on inorganic composites and hybrid membrane materials that are already in use in alternative power engineering.

DOI: 10.1134/S1070363210030473

INTRODUCTION

Ionically conducting nanocomposites find extensive technological application. At the same time, relevant studies have a comparatively brief history. In 1914, Turbandt and Lorentz discovered that, after a phase transition at 420 K, a typical ionic crystal, silver iodide, exhibited a high ionic conductivity which was earlier observed for electrolyte solutions solely [8]. It was not until a fairly long period had passed that the importance of this discovery was realized. In fact, the first systematic studies of ionic conductivity of solid electrolytes date back as far as the middle XX century.

Nearly sixty years after the Turbandt and Lorentz's discovery, Liang revealed enhancement of ionic conductivity in composites relative to their individual constituents. The conductivity of lithium iodide having a fairly low cationic mobility is enhanced by several orders of magnitude in a system comprised of LiI and finely dispersed alumina, which is a dielectric [9]. Surprisingly, a mixture of two substances that do not react with each other acquired a novel property. This discovery was comprehended by the scientific community much more rapidly, due above all to the prospects it offered for high-capacity condenser and lithium ion cell applications [10]. Subsequently, the relevant ionic conductivity studies were focused primarily on composites based on silver salts and alumina or silica. The Liang's discovery was immediately followed by numerous studies into ionic conductivity enhancement, caused by introduction into

silver, mercury, lithium, and monovalent copper halide crystals of finely dispersed inert powder, above all, alumina, silica, and titania [11–17].

This line of research is of much practical significance. Ionically conducting composites are promising candidates for numerous technical and engineering applications (gas and liquid sensors, electrochemical devices, and, above all, alternative power sources, etc.).

We present here a review of studies into ionic conductivity of nanocomposites, in particular, hybrid membrane materials, with emphasis on relevant activities by Russian researchers.

Interface Defect Formation

The processes occurring in composite electrolytes are driven by interface defects. The uncompensated and unsaturated bond system on the surface of every crystal makes it reactive toward other phases (surfaces of other solids, liquids, and gases).

Let us once again turn to a system comprised of lithium iodide and finely dispersed alumina with a developed surface. The surface sorption conditions for different cations and anions are typically non-equivalent, with a certain sort of ions being sorbed preferentially. In the LiI–Al₂O₃ system, only lithium ions exhibit mobility. Being unable for penetrating inside alumina particles, they can be actively adsorbed on alumina surface. The electrical neutrality of such systems is maintained by negatively charged cationic vacancies that are concentrated in the adjoining lithium

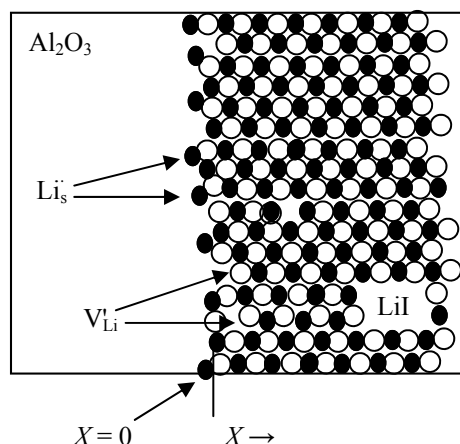
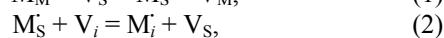


Fig. 1. Scheme of electric double layer formation at the LiI–Al₂O₃ interface.

iodide layer. This leads to formation at the LiI/Al₂O₃ interface of a ~1-μm electrical double layer.

There are not a lot of experimental facts validating this effect. For example, the IR absorption spectrum of iron hydrosulfate–silica composite does not contain a band associated with stretching vibrations of the surface OH groups weakly involved in hydrogen bonding, characteristic for the initial silica gel [19]. More active protons of hydrosulfate are partly sorbed on the silica gel surface, which leads to formation of a highly deficient interfacial layer. The sorption theory for composite electrolytes [20–30] interprets this phenomenon as sorption of cationic vacancies or interstices at the interface. The oppositely charged defects are concentrated in a narrow Debye layer near the surface. This induces the so-called surface charge which is negated in the crystal bulk [21, 31, 32]. The interface defect formation can be quantitatively interpreted as involving formation of (1) cationic vacancies V and (2) interstices i in the crystal bulk, accompanied by generation and annihilation of metal ions on the surface:



where, in Kroeger–Wink notation, the subscripts denote the cationic (M), surface (S), or interstitial siting of a metal ion or vacancy, and the superscripts indicate positive or negative charge of the species relative to the site it occupies.

Let us designate the Gibbs energy of quasichemical reactions (1) and (2) as ΔG_v and ΔG_i , respectively. At $\Delta G_v < \Delta G_i$ the interface is enriched in cations, and the

vacancy concentration in the interface vicinity increases relative to the bulk. At $\Delta G_v > \Delta G_i$ an opposite process occurs. Kliever [31] reported that defects are primarily located inside the Debye layer, within which their concentration varies from C_{v0} to $1.7C_{v\infty}$. In most of practically important situations, the thickness of this layer λ is small relative to the crystal dimension along x axis (Fig. 1) and can be calculated as

$$\lambda = (\epsilon\epsilon_0 kT / 2e^2 C_\infty)^{1/2}, \quad (3)$$

where ϵ is the relative dielectric permittivity of the material; ϵ_0 , absolute dielectric permittivity; e , electron charge; and $C_\infty = N_{v\infty} = N_{i\infty}$, defect density in the crystal bulk.

The defect concentration profile can be represented as:

$$N_v = N_{v\infty} \exp[Z], \quad (4)$$

$$N_i = N_{i\infty} \exp[-Z], \quad (5)$$

where

$$Z = 4\pi h^{-1}(\exp[-x/\lambda] \tanh[Z_0/4]), \quad (6)$$

$$Z_0 = Z(x=0) = -(\Delta G_v - \Delta G_i)/(CRT). \quad (7)$$

The electric potential difference between the bulk ($x = \infty$) and surface ($x = 0$) can be represented as

$$\phi - \phi_0 = (\Delta G_v - \Delta G_i)/(2e). \quad (8)$$

For crystals whose size is large compared to the Debye length, this is a constant parameter. The surface potential for the silver chloride (silver bromide) crystal–air interface changes from –0.1 to –0.25 eV upon heating from 298 to 550 K [33, 34]. Hence, at room temperature, the concentration of cationic interstices in these compounds exceeds that in the crystal bulk by three orders of magnitude [33].

Maier [25] described various types of interactions at solid–solid interfaces, having substantially different implications (Fig. 2). For example, in systems comprised of alumina and lithium iodide, silver chloride, or a bivalent metal fluoride, mobile monovalent ions (Li^+ , Ag^+ , F^-) are adsorbed at the interface, with the vacancy concentration increasing in the Debye layer (Figs. 2a, 2b) [26, 35]. Interaction of the silver chloride crystal surface with ammonia vapor leads to an increase in the cationic vacancy concentration via sorption of NH_3 molecules at the interface with formation of relatively strong complexes with silver ions (Fig. 2c) [25]. By contrast, reactions of silver chloride or calcium fluoride with Lewis bases (BF_3 or AsF_5) yield strong anionic complexes on the surface. This is accompanied

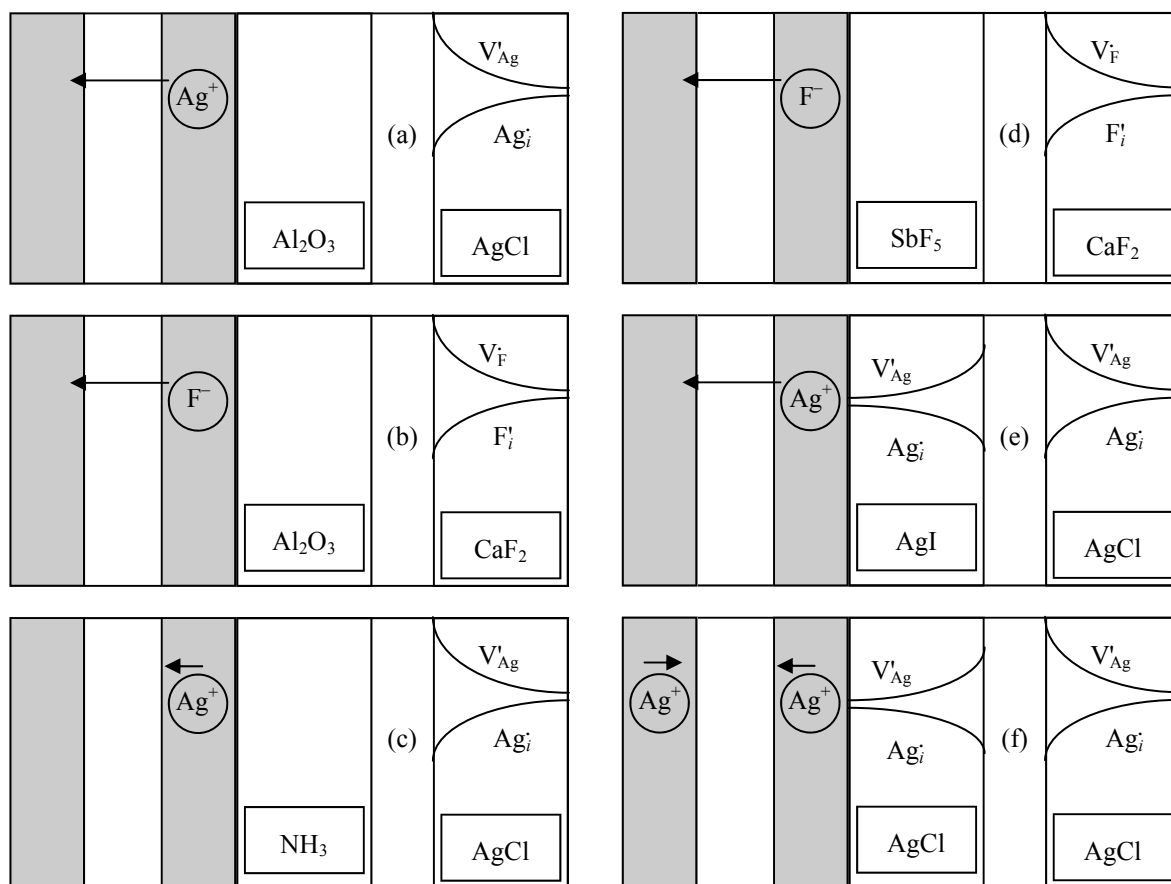


Fig. 2. Scheme of formation and variation of concentration of defects at interfaces along the sample length in (a) AgCl/Al₂O₃, (b) CaF₂/Al₂O₃, (c) AgCl/NH₃, (d) CaF₂/SbF₅, (e) AgI/AgCl, and (f) polycrystalline AgCl (AgCl/AgCl) composite system.

by a sharp increase in concentration of silver cations in interstices and of vacancies at fluoride sites within the Debye layer (Fig. 2d) [25, 27, 36]. However, interaction of β -modification of silver iodide with silver bromide or silver chloride containing similar cations also leads to a significant conductivity enhancement [37, 38]. The reason lies in the difference between the chemical potentials of silver in AgI and AgCl crystals (Figs. 2e, 2f).

Ionic Conductivity of Composites

Most of currently available models describe the electrical conductivity of composite materials in the approximation of series- and parallel-connected elements with different resistances [39–41]. The solution of the problem is typically reduced to determining the conductivity σ_{tot} for a system comprised of two individual phases with conductivities σ_1 and σ_2 and volume fractions $(1 - \eta_2)$ and η_2 , respectively. The simplest models can be found in systems with series-

and parallel-connected conducting segments whose conductivity is determined as

$$\Sigma_{\text{tot}}^{-1} = (1 - \eta_2)\sigma_1^{-1} + \eta_2\sigma_2^{-1}, \quad (9)$$

$$\sigma_{\text{tot}} = (1 - \eta_2)\sigma_1 + \eta_2\sigma_2. \quad (10)$$

These simple models can predict the lower and upper conductivity limits for composite materials. Real systems comprised by alternating series- and parallel-connected particles are described by intermediate versions.

However, all these models cannot explain a sharp increase in conductivity of composites relative to those of their constituents. Stoneham et al. [42] presumed that formation of a high-conductivity phase is associated with water sorption. Jow and Wagner [12] attributed the conductivity enhancement in MI–Al₂O₃ binary systems to an increase in defect concentration for salts containing mobile M^+ ions. This hypothesis specifically underlies modern transport theories as applied to composite materials.

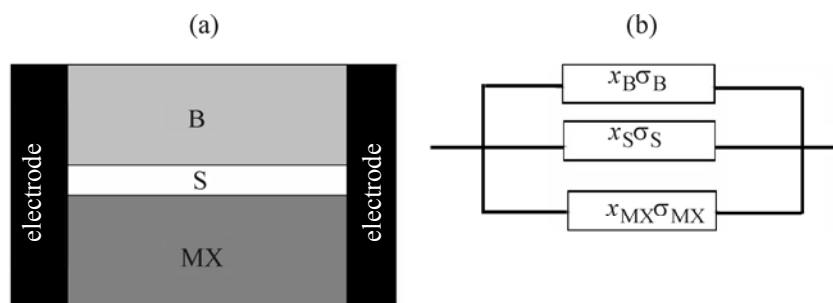


Fig. 3. (a) Schematic structure and (b) equivalent electric circuit for a “bicrystal” comprised of ionic crystal MX, an inert phase B, and a highly defective layer S at their interface.

As known, transport processes in solids are driven by defect migration exclusively [43]. Hence, the conductivity of a material can be represented as the defect concentration C_D multiplied by the defect mobility μ_D :

$$\sigma = C_D \mu_D. \quad (11)$$

At the interface, the defect concentration can increase by several orders of magnitude. Also, uncompensated valence bonds and weaker steric hindrance to transport in the subsurface layer are responsible for the ionic mobility at interfaces being typically much higher than in the bulk. Increases in both multipliers on the right-hand side of Eq. (11) lead to enhancement of ionic conductivity near interfaces in composites.

Let us consider the model suggested by Maier [21, 44] as applied to interaction of two single crystals MX (ionic crystal) and B (inert nonconductive phase). The corresponding scheme shows that the interface is parallel to the potential difference vector (Fig. 3a).

The total conductivity of this system can be represented as the sum of three components corresponding to three parallel-connected resistances

$$\sigma_{\text{tot}} = X_B \sigma_B + X_{MX} \sigma_{MX} + X_S \sigma_S, \quad (12)$$

where X and σ are the volume fraction and conductivity of each of the components, respectively; $X_B \sigma_B$ and $X_{MX} \sigma_{MX}$, contributions from conductivities of the inert phase and ionic crystals MX, respectively; and $X_S \sigma_S$, contribution from conductivity of the surface charged layer in MX. The contribution from the inert phase, $X_B \sigma_B$, is typically negligible. As to the two remaining terms, $X_{MX} \sigma_{MX}$ dominates for large, and $X_S \sigma_S$, for small crystals.

Having integrated the defect concentration profile, Maier obtained a fairly simple expression describing

the contribution from the surface component to the ionic conductivity of the material:

$$X_D \sigma_D \approx q u_v (2\lambda) (C_{vb} C_{vi})^{1/2}, \quad (13)$$

where q and u_v are the vacancy charge and mobility, respectively, and C_{vb} and C_{vi} , vacancy concentration in the crystal bulk and at the interface, respectively.

Thus, the contribution to conductivity from the Debye layer can be represented by means of a parallel-connected resistance with the thickness 2λ and a certain averaged concentration of carriers near the interface, determining its conductivity (see Fig. 3a).

Real objects are typically represented by polycrystalline systems comprised of a multitude of conductive and nonconductive crystals and their interfaces. In the simplest case, the conductivity of a polycrystalline sample consisting of numerous small cubic crystals with the edge length L can be described in terms of the cubic block model (Fig. 4). Under $L \gg 2\lambda$ presumption, it is possible to neglect a minor contribution to the conductivity from the layers perpendicular to the potential difference vector. Then, the ratio of the contributions to the total system conductivity from the block-crystal bulk interfaces can be represented as:

$$X_{MX} \sigma_{MX} / X_S \sigma_S = (L - 2\lambda) X_{MX} / 2\lambda X_S. \quad (14)$$

In the case of real heterogeneous systems, the calculation of conductivity is a much more complicated task because of diversified topological distribution of two (more precisely three) phases (including the highly deficient Debye layer) [45–47].

The Monte Carlo simulation of the conductivity of LiI–Al₂O₃ binary system in terms of the percolation model [46, 48] yielded the following results, as exemplified by a two-dimensional model shown in

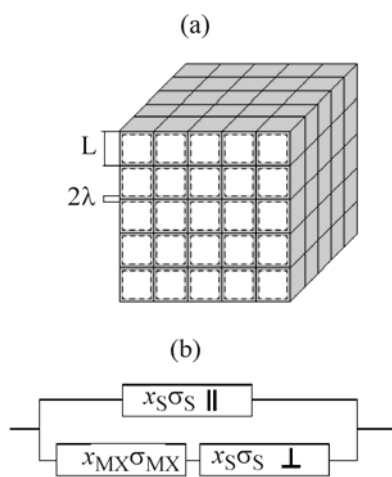


Fig. 4. (a) Cubic block model and (b) equivalent electrical circuit for a polycrystalline sample. The high-conducting Debye layer is shown in grey.

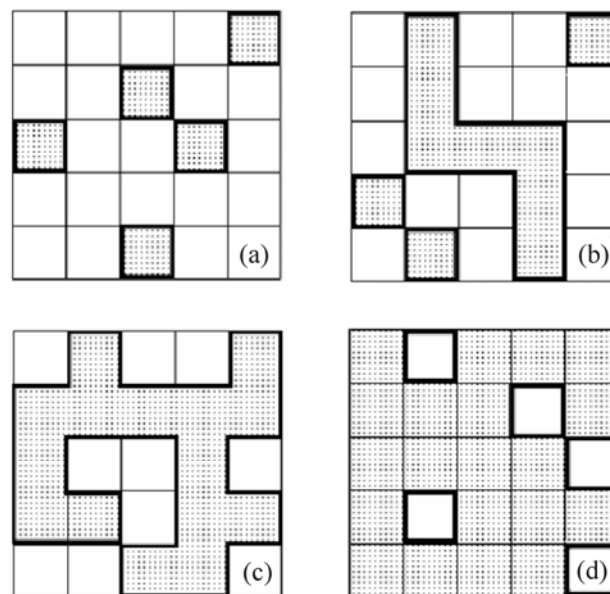


Fig. 5. (a)–(d) Scheme of formation of highly-conducting chains in a solid composite electrolyte with progressively increasing content of inert phase.

Fig. 5. At low oxide phase concentrations the conductivity increases because of appearance of highly conducting contacts (Fig. 5a). At inert phase concentrations above which the oxide particles are in permanent contact (first percolation threshold), highly conducting chains are formed (Fig. 5b). The second percolation threshold is achieved at the inert phase concentration above which the highly conducting chains are broken (Fig. 5c). Between these critical points the conductivity of the system varies fairly insignificantly, being close to a maximum. Upon passing through the second critical concentration the conductivity of the system rapidly decreases and tends to zero (Fig. 5d). This approach was employed for describing the concentration dependence of the conductivity for a series of systems comprised of lithium or silver salts and various oxide additions [49]. The blocking effect is of greatest significance for superionic salts [50] and systems containing ionic crystals characterized by a fairly high intrinsic defectiveness [51].

A typical conductivity–composition plot for composite electrolytes passes through a maximum at the highly dispersed oxide phase content ranging from 20 to 40% (Fig. 6).

For most of solid electrolytes the temperature dependence of ionic conductivity is described by the Frenkel equation

$$\sigma T = A \exp(-E\sigma/kT). \quad (15)$$

where A is the pre-exponential coefficient, and E_σ , conduction activation energy. For neat binary crystals AX the activation energy is equal to the sum of the defect mobility activation energy E_a and the halved enthalpy of defect formation ΔH :

$$E\sigma = E_a + 1/2\Delta H. \quad (16)$$

Heterogeneous doping of ionic crystals leads to a decrease in the conduction activation energy. The parameter ΔH for composites is equal to the enthalpy of defect formation at the interface, which is considerably lower than that in undoped crystal. When the enthalpy of ion sorption at the interface is negative and fairly large in modulus, sorption is weakly temperature-dependent, and the conduction activation energy tends to E_a . Thus, at low temperatures, the conductivity of heterogeneous systems increases, and the conductance activation energy, decreases (Fig. 7, curves 1–3) [21, 48, 53, 54]. However, the intrinsic conductivity, being weakly dependent on the heterogeneous doping level, increases much faster with increasing temperature because of a higher activation energy. This is responsible for its typical dominance at high temperatures. In the high-temperature region, a low-conducting impurity may cause, by contrast, a decrease in conductivity. This effect is most pronounced in compounds exhibiting a superionic transition accompanied by an increase in intrinsic dis-

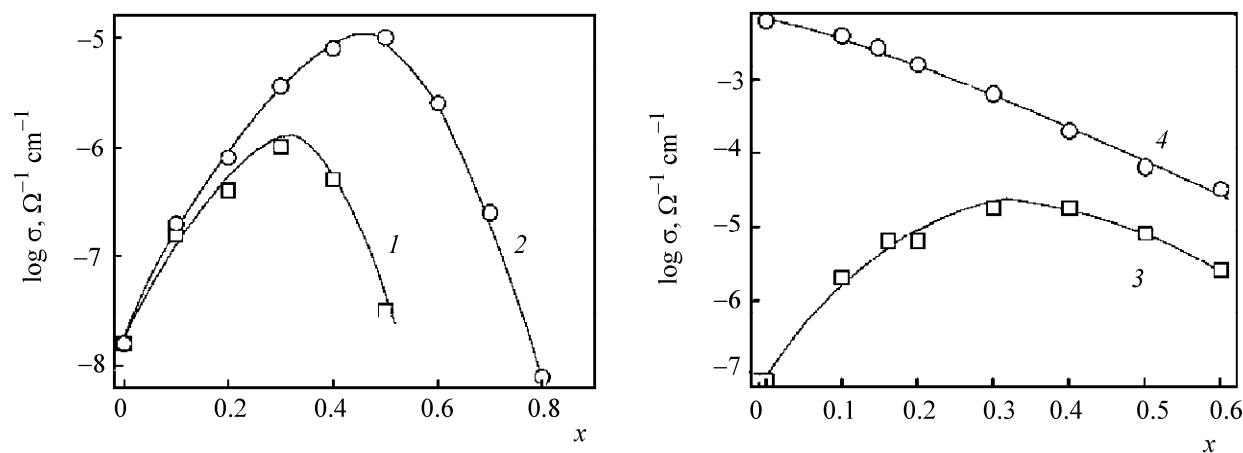


Fig. 6. Conductivity–composition plots for composite systems: (1) $(1-x)\text{Li}_2\text{CO}_3 \cdot x\text{Al}_2\text{O}_3$, (2) $(1-x)\text{Li}_2\text{CO}_3 \cdot x\text{BaTiO}_3$ at 250°C [52], and (3, 4) $(1-x)\text{CsHSO}_4 \cdot x\text{TiO}_2$ at (3) 80 and (4) 170°C [50].

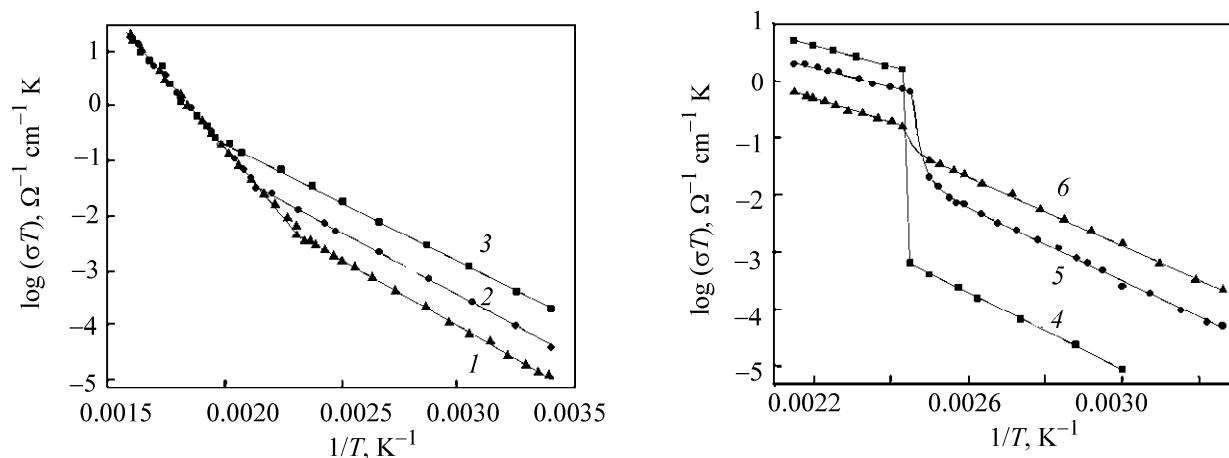


Fig. 7. Temperature dependence of conductivity, represented in the Frenkel equation (16) coordinates for (1–3) $(1-x)\text{CuBr} \cdot x\text{TiO}_2$ [54] and (4–6) $(1-x)\text{CsHSO}_4 \cdot x\text{TiO}_2$ [50] composites with x of (1, 4) 0, (2) 0.199, (5) 0.2, (3) 0.212, and (6) 0.5.

ordering of crystals. In that case, the presence of a heterogeneous impurity leads to an increase in conductivity and a decrease in conduction activation energy at low temperatures. By contrast, at high temperatures the conductivity decreases and the conduction activation energy remains unchanged or slightly increases. These trends were also observed for $\text{AgI}-\text{I}_2\text{O}_3$ [55], $\text{CsHSO}_4-\text{iO}_2$ [56–59], and $\text{CsHSO}_4-\text{TiO}_2$ [50] systems (Fig. 7, curves 4–6).

Why, Specifically, Nanocomposites?

The subtitle question with the word “composites” removed belongs to a group of rhetorical questions that have been posed in recent years. This question has a very simple answer which is evident from the above

discussion: Since the conductivity enhancement for composite materials is driven specifically by interfaces, the higher the proportion of interfaces, the higher the conductivity of a system. Considering the fact that the Debye layer thickness is governed by the nature of the initial components solely, this implies the following: The smaller their particles, the larger the specific surface area of interface. Equation (16) suggests that the contribution to the total conductivity from interfaces steadily increases with decreasing particle size.

Thus, size-dependent effect in conductivity of solid composite electrolytes has a very simple explanation. For larger particles, the composition has a negligible effect compared to bulk conductivity, while for small particles

the conductivity can be virtually entirely determined by the surface properties. Moreover, with particle size reduction to nanoscale the boundaries of highly defective Debye layers can overlap, which will render highly conductive the entire nanoparticle [60].

Studies of hydrogen phosphates and sulfates of polyvalent metals as examples revealed the following. The protonic conductivity of systems comprised of large particles is independent of the particle size. When the particle size decreases beyond 100 nm, the protonic conductivity rapidly increases (Fig. 8). This trend is explained by an increase in the surface proportion with decreasing particle size. Also, ions from deep-lying layers are involved in mobility by the surface ions exhibiting enhanced mobility. An NMR examination of a zirconium hydrogen phosphate crystal showed that the proportion of mobile (surface) ions tends to increase with increasing temperature [61]. This trend is even more pronounced in composites comprising the second phase that typically exhibits a high sorption activity.

Studies of ionic conductivity and thermodynamic properties of nanocomposites showed that the physical properties of ionic salts in composite systems considerably differ from those of individual compounds [55, 62–66]. At high concentration and high dispersity of the oxide phase, the formation of the composite is accompanied by MX salt dispersion of via solid-phase “spreading” over the oxide surface. In the limiting case, the salt can virtually exhaustively pass to the so-called “surface” state. Formation of a surface phase with high mobility in composite materials was also supported by relevant NMR data [67]. Another validation can be found in decreases in the endothermic effect accompanying the superionic phase transition and in the temperature of this transition, observed for some ionic salts (Li_2SO_4 , AgBr , AgI , CsHSO_4 , and RbHSO_4) constituting the composite matrix. At a high content of the oxide component, no phase transition is observed [50, 55, 56–58, 68, 69]. Thus, a new superionic phase characterized by high cationic disordering is formed at interfaces between particles in the composite.

It was also shown [50, 52, 53, 70] that the properties of composite electrolyte are strongly affected by the degree of dispersity of the oxide phase. With increasing dispersity, the influence exerted by the oxide phase on the electrical conductivity of the composite and on ion current blocking is enhanced [49]. It

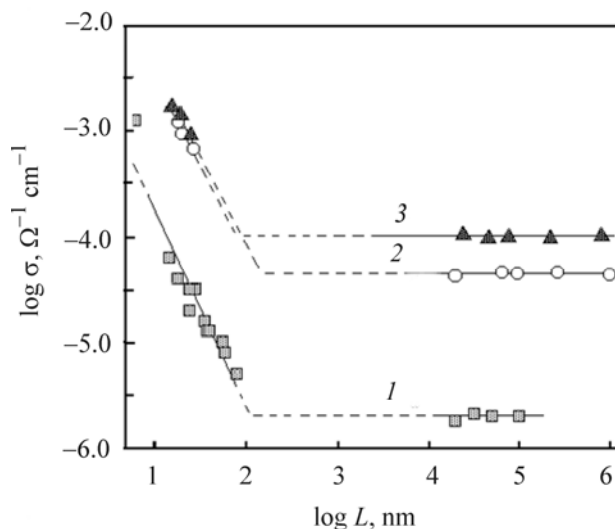


Fig. 8. Electrical conductivity measured in the direction perpendicular to z crystallographic axis vs. particle size for (a) $\text{Zr}(\text{HPO}_4)_2 \cdot \text{H}_2\text{O}$, (b) $\text{Fe}(\text{HSO}_4)_2 \cdot 4\text{H}_2\text{O}$, and (c) $\text{InH}(\text{SO}_4)_2 \cdot 4\text{H}_2\text{O}$ [61].

should also be noted that the pore size of the oxide phase also strongly affects the properties of composites because of the changes in sorption activity of the pores with respect to various cations and dispersing ability with respect to ionic salts. For example, a maximal increase in conductivity for $\text{MHSO}_4\text{--SiO}_2$ composites can be achieved at the pore size of 35–100 Å [57–59].

Main Lines of Conductivity Research for Inorganic Composites

Major views of the transport properties of composites have already been shaped by now. The emphasis in relevant studies is further placed on broadening the spectrum of composite materials covered. Along with traditionally examined lithium, copper, and silver chlorides, bromides, and iodides, significant developmental efforts are devoted to systems containing lithium salts, in particular, fluoride [53], carbonate [52, 53, 71], sulfate [68, 72], perchlorate [73], and phosphate [53]. Much attention is paid to composites based on alkali metal nitrates [62, 64, 74–77], as well as to composites containing other cationically conducting salts, in particular, silver sulfate [78], sodium carbonate [79], cesium chloride [66], etc. Among anionically conducting composites, the focus is on those based on calcium [27, 36, 80] and lead halides [26, 35].

Also, special mention should be made of studies that revealed formation of surface phases with unusual

transport properties in calcium tungstate- and WO_3 -based ceramic composites [81, 82].

Much effort was dedicated to improving the properties of protonically conducting solid electrolytes. Indeed, a high polarizing effect must be responsible for active sorption of protons at interfaces with various oxide phases. In this connection, attempts were made to increase the conductivity of hydrated antimony oxide [83], zirconium hydrogen phosphate [84, 85], and heteropoly acids [86] by doping finely dispersed oxides of polyvalent elements and zeolites. However, those attempts were unsuccessful. The main reason lies in high intrinsic disordering in the materials chosen for these experiments, in which situation heterogeneous additions are of little use for improving the properties of these materials.

Much progress was achieved in stabilization of highly conducting phase of cesium, rubidium, potassium, and ammonium hydrogen sulfates by doping highly dispersed silica and titania [56–58, 87–91]. Also, some other relevant studies deserve mentioning [92–94]. The protonic conductivity of iron and indium hydrogen sulfates was significantly increased by doping finely dispersed silica and zirconia [19, 95, 96]. Relevant IR spectroscopic studies showed that this effect was achieved via sorption of protons from acid groups on silica gel [19].

Much searching activity is undertaken with respect to composite solid electrolytes based on hydrogen phosphates, in particular, cesium hydrogen phosphate [97], and mixed cesium sulfate-phosphate [98, 99]. New composite electrolytes were prepared on the basis of $\text{TaH}(\text{PO}_4)_2 \cdot 2\text{H}_2\text{O}$ and SiO_2 [100].

A large interfacial area in composites is typically achieved when one or both substances are introduced in the nanodispersed state, which is followed by heat treatment of the resulting material at a high temperature, close to or even exceeding the melting point of the ion-conducting component. Recent years have witnessed active use of physical or chemical approaches in the search for alternative nanocomposite formation routes. For example, a new technique was suggested for increasing the ionic conductivity of solid electrolytes by chemical modification of their surface [101]. For example, a thin nanometer-thick layer of the ion-exchange products on the surface of zirconium hydrogen phosphate crystals leads to a sharp increase in conductivity of the system. It should be noted that the layer thickness does not exceed that of the highly

deficient Debye layer. With increasing degree of substitution this layer is blocked by exchange products, which causes the conductivity of the system to decrease [102].

A conceptually similar and very interesting approach to nanocomposite formation implies successive deposition of calcium and barium fluoride layers [103, 104].

Also, nanocomposites were prepared by introducing silver iodide into porous alumina [105], as well in mesoporous oxides characterized by ordered arrangement of nanosized (2–10-nm) pores [106].

Hybrid Membrane Materials

Heterogeneous composition and flexible polymer chains of ion-exchange membranes based on macromolecular compounds predetermine their specific structural features of which heterogeneity is the most important [107]. It is manifested in the occurrence in such membranes of segments dominated by hydrophobic moieties (hydrocarbon chains, aromatic groups, perfluorinated chains). Hydrophilic functional groups form nanosized clusters inside the membranes.

Gierke et al. [108–110] deduced a heterogeneous structure of these membranes from analysis of small-angle reflections in X-ray diffraction patterns and presumed a close-to-spherical shape for the cluster. Hydration of membranes leads to an increase in the cluster size, associated both with increased number of functional groups and additional water molecules embedded into the membrane [108, 111]. In terms of this model, the transport through the membrane is described with the use of narrow channels integrating individual clusters into a single network.

Heterogeneous structure of the membranes was also detected with small-angle X-ray scattering technique [110, 112, 113], Mössbauer [114] and nuclear magnetic resonance [115] spectroscopy, porosimetry, electron microscopy [116], differential scanning microscopy, etc. [127, 128].

The existing ion-exchange membranes do not fully satisfy the steadily increasing demands, above all in terms of thermal stability and transport properties. This motivated intensification of efforts that have been recently focused on modification of membrane materials and preparation of hybrid membranes containing inorganic and macromolecular components [107, 119, 120].

The macromolecular components in these membrane materials are represented by reactive ion-exchange membranes able of sorbing both cations [121–123] and anions [124]. Suitable for these purposes is a broad spectrum of inorganic dopants, in particular, hydrated oxides of polyvalent elements (aluminum, silicon, titanium, zirconium, hafnium, tantalum, tungsten, antimony) [121, 125–130], zeolites and clay minerals [131, 132], heteropoly acids [122, 133–137], and acid salts [123, 138–142]. The characteristic size of the embedded particles ranges from several nanometers to several hundreds of nanometers [133]; in most cases, they form individual islands in membranes [143, 144]. Composite membranes are beneficial in terms of improved mechanical properties, selectivity, and enhanced (in some of these systems) ionic conductivity. For example, in certain cases composite materials of this type have an ionic conductivity of 10^{-3} – 0.2 S cm^{-1} . Noteworthy, these systems exhibit enhanced conductivity at low humidities [121, 124, 127, 140, 145].

There exist two principally possible routes for modification of membrane materials with nanoparticles: solution-casting of membranes with the use of finely dispersed dopants and nanoparticle synthesis in membrane matrix [119].

Membranes offer unique matrices for nanoparticle synthesis. Their nanopores are able of efficiently sorbing one of the reactants, e.g., cations in the case of cationic membranes. Subsequently, nanoparticles can be synthesized in the same nanopores (acting as peculiar nanoreactors), thereby limiting the amount of the reactants spent. Lastly, the resulting particle can be efficiently isolated from one another by the membrane walls, so that the surface tension will be decreased and thermodynamic stability of the particles will be provided. This technique was applied for synthesizing materials containing nanosized silica, zirconia, and zirconium hydrogen phosphate particles [144, 146–148]. The resulting particles (detected by electron microscopy, X-ray phase and microprobe analyses, and high-resolution NMR spectroscopy) measured several nanometers in size, which corresponds to the pore size in the initial membrane (Fig. 9).

The composite membranes prepared by this technique possess a set of practically valuable properties, e.g., increased protonic conductivity in many cases. Some of the materials exhibit significantly enhanced ion-transport selectivities, as suggested by manifold

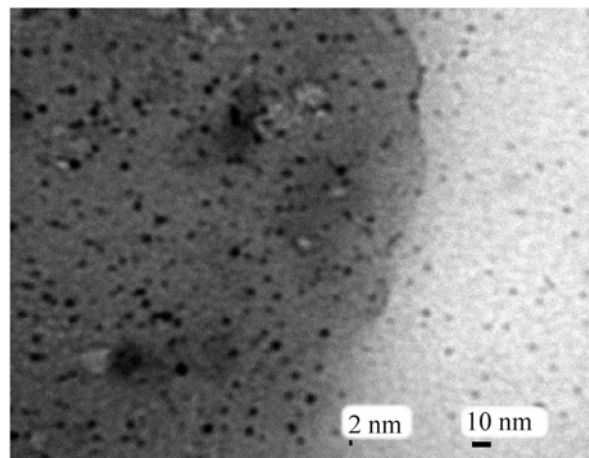


Fig. 9. Electron image of MF-4SK membrane with *in situ* synthesized hydrated silica [144].

decrease in the anion transport number [147]. The same technique was applied for preparing membranes characterized by gradient distribution of dopant particles, which exhibited diffusion permittivity anisotropy [144, 149].

Radiation-chemical grafting of vinylidene chloride to MF-4SK perfluorinated sulfocationic membrane, followed by dehydrochlorination of grafted polymer, yielded carbon nanoparticle-modified membranes [150]. Compared to the initial membrane, the synthesized material exhibit ionic-electronic conductivity, but has a slightly lower protonic conductivity.

Of much interest are the experiments on modification of MF-4SK perfluorinated membranes with polyaniline. A composite was synthesized both by aniline polymerization in the membrane matrix and in MF-4SK solutions, followed by membrane casting [151–158]. In the latter case the polyaniline particle size was not limited by the pore size and ranged from several nanometers to several tens of nanometers [151]. It was shown [152] that the electronic conductivity can contribute with 60–70% to the total electrical conductivity of those composites. As to protonic conductivity of the composites prepared by aniline polymerization in an MF-4SK solution, it passes through a maximum at a close to 0.05 ratio of the number of nitrogen atoms in polyaniline to that of sulfo groups in MF-4SK [151]. Also, such membranes are characterized by decreased water transport numbers [152–154].

CONCLUSIONS

Synthesis of ionically conducting composite materials not only is a matter of academic interest but also represents one of the major lines of research in modern electrochemistry. Early stages of studies into ionic conductivity phenomenon, which have a brief history of 35 years only, were focused on inorganic composites. For them, a fairly coherent theory was developed which interprets the nature of the phenomenon but not always provides a correct quantitative description thereto. Recently, emphasis has been placed on synthesis and study of hybrid membrane materials based on macromolecular ion-exchange membranes and nanodispersed inorganic dopants. These systems showed good results in hydrogen power engineering applications, which is widely believed to be a promising solution to many environmental problems. At the same time, the processes occurring in hybrid membranes are considerably different from those in inorganic composites and need special examination.

REFERENCES

1. European Commission. *Eur20719 EN – Hydrogen Energy and Fuel Cells – A Vision of Our Future*, Luxembourg: Office for Official Publications of the European Committees, 2003.
2. Mesyats, G.A. and Prokhorov, M.D., *Vestn. Ross. Akad. Nauk*, 2004, vol. 74, p. 579.
3. Kuzyk, B.N., *Rossiia i mir v XXI veke* (Russia and the World in the XXI Century), Moscow: Inst. Ekon. Strat., 2005.
4. Kreuer, K.-D., Paddison, S.J., Spohr, E., and Schuster, M., *Chem. Rev.*, 2004, vol. 104, pp. 4637–4679.
5. Hickner, M.A., Ghassemi, H., Kim, Y.S., Einsla, B.R., and McGrath, J.E., *Chem. Rev.*, 2004, vol. 104, pp. 4587–4612.
6. *Vision for Nanotechnology Research and Development in the Next Decade*, Roco, M.C., Williams, S., and Alivisatos, P., Eds., Dordrecht: Kluwer, 2000.
7. Poole, C.P., Jr. and Owens, F.J., *Introduction to Nanotechnology*, New York: Wiley, 2003.
8. Turbandt and Lorentz, E., *Z. Phys. Chem.*, 1914, vol. 87, pp. 513–517.
9. Liang, C.C., *J. Electrochem. Soc.*, 1973, vol. 120, pp. 1289–1292.
10. Liang, C.C., Joshi, A.V., and Hamilton, N.E., *J. Appl. Electrochem.*, 1978, vol. 8, pp. 445–449.
11. Crosbie, G., *J. Solid State Chem.*, 1978, vol. 25, pp. 1978–1982.
12. Jow, T. and Wagner, J.B., *J. Electrochem. Soc.*, 1979, vol. 126, pp. 1963–1972.
13. Pack, S., Owens, B., and Wagner, J.B., *J. Electrochem. Soc.*, 1980, vol. 127, pp. 2177–2179.
14. Skarstad, P., Merritt, D.B., and Owens, B.B., *Solid State Ionics*, 1981, vols. 3–4, pp. 277–281.
15. Shahi, K. and Wagner, J.B., *Solid State Ionics*, 1981, vols. 3–4, pp. 295–299.
16. Shahi, K. and Wagner, J.B., *J. Electrochem. Soc.*, 1981, vol. 128, pp. 6–13.
17. Nakamura, O. and Goodenough, J.B., *Solid State Ionics*, 1982, vol. 7, pp. 119–123.
18. Petrii, O.A., *Electrochim. Acta*, 1996, vol. 41, pp. 2307–2312.
19. Ponomareva, V.G., Tarnopol'skii, V.A., Burgina, E.B., and Yaroslavl'tsev, A.B., *Zh. Neorg. Khim.*, 2003, vol. 48, pp. 1061–1066.
20. Jamnik, J. and Maier J., *Solid State Ionics*, 1997, vol. 94, pp. 189–198.
21. Maier, J., *J. Phys. Chem. Solids*, 1985, vol. 46, pp. 309–320.
22. Maier, J., *Ber. Bunsenges. Phys. Chem.*, 1989, vol. 93, pp. 1468–1473.
23. Maier, J., *Solid State Ionics*, 1994, vol. 70, pp. 43–51.
24. Jamnik, J., Habermeier, H.U., and Maier J., *Physica B*, 1995, vol. 204, pp. 57–64.
25. Maier, J. *Solid State Ionics*, 1995, vol. 75, pp. 139–145.
26. Hariharan, K. and Maier, J., *J. Electrochem. Soc.*, 1995, vol. 142, pp. 3469–3473.
27. Saito, Y. and Maier, J., *Solid State Ionics*, 1996, vols. 86–88, pp. 581–584.
28. Jamnik, J. and Maier, J., *J. Electrochem. Soc.*, 1998, vol. 145, pp. 1762–1767.
29. Jamnik, J. and Maier, J., *J. Phys. Chem. Solids*, 1998, vol. 59, pp. 1555–1559.
30. Maier, J., *Solid State Ionics*, 2000, vol. 131, pp. 13–18.
31. Kliever, K.L., *J. Phys. Chem. Solids*, 1966, vol. 27, pp. 705–710.
32. Yaroslavl'tsev, A.B., *Rus. J. Inorganic Chem., Suppl.* 3, 2001, vol. 46, pp. S249–S267.
33. Wonnell, S.K. and Slifkin, L.M., *Solid State Ionics*, 1995, vol. 75, pp. 101–106.
34. Wonnell, S.K. and Slifkin, L.M., *Phys. Rev. B.*, 1993, vol. 48, pp. 78–83.
35. Kumar, A. and Shahi, K., *J. Mater. Sci.*, 1993, vol. 28, pp. 1257–1263.
36. Saito, Y. and Maier, J., *J. Electrochem. Soc.*, 1995, vol. 142, pp. 3078–3083.
37. Lauer, U. and Maier, J., *Ber. Bunsenges. Phys. Chem.*, 1992, vol. 96, pp. 111–119.
38. Lauer, U. and Maier, J., *Solid State Ionics*, 1992, vol. 51, pp. 209–213.

39. Landau, L.D. and Lifshitz, E.M., *Electrodynamics of Continuous Media*, Oxford: Pergamon, 1960.
40. Bunget, I. and Popescu, M., *Physics of Solid Dielectrics*, Elsevier: Romania, 1984.
41. Han, D.G. and Choi, G.M., *Solid State Ionics*, 1998, vol. 106, pp. 71–87.
42. Stoneham, A.M., Wade, E., and Kilner, J.A., *Mater. Res. Bull.*, 1979, vol. 14, pp. 661–666.
43. Bokshstein, B.S. and Yaroslavstev, A.B., *Diffuziya atomov i ionov v tverdykh telakh* (Diffusion of Atoms and Ions in Solids), Moscow: Mosk. Inst. Stali Splav., 2005.
44. Maier, J., *Prog. Solid State Chem.*, 1995, vol. 23, pp. 171–263.
45. Bunde, A., Dieterich, W., and Roman, H.E., *Phys. Rev. Lett.*, 1985, vol. 55, pp. 5–8.
46. Roman, H.E., Bunde, A., and Dieterich, W., *Phys. Rev. B*, 1986, vol. 34, pp. 3439–3448.
47. Dieterich, W., Durr, O., Pendzig, P., Bunde, A., and Nitzan, A., *Physica A*, 1999, vol. 266, pp. 229–237.
48. Bunde, A., *Solid State Ionics*, 1995, vol. 75, pp. 147–155.
49. Uvarov, N.F., Vanek, P., Savinov, M., Zelezny, V., Studnicka, V., and Petzelt, J., *Solid State Ionics*, 2000, vol. 127, pp. 253–267.
50. Ponomareva, V.G. and Lavrova, G.V., *Solid State Ionics* 1997, vol. 106, pp. 137–141.
51. Kleitz, M., Dessemond, L., and Steil, M.C., *Solid State Ionics*, 1995, vol. 75, pp. 107–115.
52. Bhoga, S.S. and Singh, K., *Solid State Ionics*, 1998, vol. 115, pp. 85–92.
53. Uvarov, N.F., Isupov, V.P., Sharma, V., and Shukla, A.K., *Solid State Ionics*, 1992, vol. 51, pp. 41–52.
54. Knauth, P., Debierre, J.-M., and Albinet, G., *Solid State Ionics*, 1999, vol. 121, pp. 101–106.
55. Uvarov, N.F., Hairetdinov, E.F., Bokhonov, B.B., and Bratel, N.B., *Solid State Ionics*, 1996, vols. 86–88, pp. 573–576.
56. Ponomareva, V.G., Uvarov, N.F., Lavrova, G.V., and Hairetdinov, E.F., *Solid State Ionics*, 1996, vol. 90, pp. 161–166.
57. Ponomareva, V.G., Lavrova, G.V., and Simonova, L.G., *Solid State Ionics*, 1999, vol. 118, pp. 317–323.
58. Ponomareva, V.G., Lavrova, G.V., and Simonova, L.G., *Solid State Ionics*, 1999, vol. 119, pp. 295–299.
59. Ponomareva, V.G., Lavrova, G.V., and Simonova, L.G., *Neorg. Mater.*, 1998, vol. 34, pp. 1347–1352.
60. Maier, J., Prill, S., and Reichert, B., *Solid State Ionics*, 1988, vols. 28–30, pp. 28–30.
61. Yaroslavl'tsev, A.B., Mirak'yan, A.L., Chuvaev, V.F., and Sokolova, L.N., *Zh. Neorg. Khim.*, 1997, vol. 42, pp. 900–904.
62. Uvarov, N.F., Vanek, P., Yuzuyk, Yu.I., Studnicka, V., Bokhonov, B.B., Dulepov, V.E., and Petzelt, J., *Solid State Ionics*, 1996, vol. 90, pp. 201–207.
63. Uvarov, N.F. and Ponomareva, V.G., *Dokl. Ross. Akad. Nauk*, 1996, vol. 351, pp. 358–360.
64. Uvarov, N.F., Hairetdinov, E.F., and Skobelev, I.V., *Solid State Ionics*, 1996, vols. 86–88, pp. 577–580.
65. Uvarov, N.F. and Vanek, P., *J. Mater. Synth. Proc.*, 2000, vol. 8, pp. 319–326.
66. Uvarov, N.F., Brezhneva, E.F., and Hairetdinov, E.F., *Solid State Ionics*, 2000, vols. 136–138, pp. 1273–1278.
67. Asai, T., Hu, C.H., and Kawai, S., *Mater. Res. Bull.*, 1987, vol. 22, pp. 269–274.
68. Uvarov, N.F., Bokhonov, B.B., Isupov, V.P., and Hairetdinov, E.F., *Solid State Ionics*, 1994, vol. 74, pp. 15–27.
69. Lee, J.-S., Adams, S., and Maier J., *J. Electrochem. Soc.*, 2000, vol. 147, pp. 2407–2418.
70. Tadanaga, K., Imai, K., Tatsumisago, M., and Minami, T., *J. Electrochem. Soc.*, 2002, vol. 149, pp. A773–A777.
71. Heitjans, P. and Indris, S., *J. Phys.: Condens. Matter.*, 2003, vol. 15, pp. R1257–R1289.
72. Uvarov, N.F., Shrivastava, O.P., and Hairetdinov, E.F., *Solid State Ionics*, 1989, vol. 36, pp. 39–42.
73. Vinod, M.P. and Bahnmann, D., *J. Solid State Electrochem.*, 2002, vol. 6, pp. 498–501.
74. Uvarov, N.F., Skobelev, I.V., Bokhonov, B.B., and Hairetdinov, E.F., *J. Mater. Synth. Proc.*, 1996, vol. 4, pp. 391–395.
75. Ponomareva, V.G., Lavrova, G.V., and Simonova, L.G., *Solid State Ionics*, 2000, vols. 136–138, pp. 1279–1284.
76. Lavrova, G.V., Ponomareva, V.G., and Uvarov, N.F., *Solid State Ionics*, 2000, vols. 136–138, pp. 1285–1290.
77. Anantha, P.S. and Hariharan, K., *J. Phys. Chem. Solids*, 2003, vol. 64, pp. 1131–1137.
78. Singh, K., Randhawa, J., Khadakkar, P., and Bhoga, S.S., *Solid State Ionics*, 1999, vol. 126, pp. 47–53.
79. Singh, K., Ambekar, P., and Bhoga, S.S., *Solid State Ionics*, 1999, vol. 122, pp. 191–196.
80. Khandkar, A., Tare, V.B., and Wagner, J.B., *Rev. Chem. Miner.*, 1986, vol. 23, pp. 274–280.
81. Konisheva, E., Neiman, A., and Gorbunova, E., *Solid State Ionics*, 2003, vol. 157, pp. 45–49.
82. Neiman, A.Ya., Pestereva, N.N., Sharafutdinova, A.R., and Kostikov, Yu.P., *Elektrokhimiya*, 2005, vol. 41, pp. 680–693.
83. Hix, G.B., Rouillard, Y., Slade, R.C.T., and Ducourant, B., *J. Mater. Chem.*, 1994, vol. 4, pp. 1921–1926.
84. Slade, R.C.T. and Knowles, J.A., *Solid State Ionics*, 1991, vol. 46, pp. 45–51.
85. Slade, R.C.T., Jinku, H., and Knowles, J.A., *Solid State Ionics*, 1992, vol. 50, pp. 287–290.

86. Tatsumisago, M., Sakai, Y., Honjo, H., and Minami, T., *J. Ceram. Soc. Jpn.*, 1995, vol. 103, pp. 189–190.
87. Ponomareva, V.G. and Lavrova, G.V., *Solid State Ionics*, 2001, vol. 145, pp. 197–204.
88. Ponomareva, V.G., Merinov, B.V., and Lavrova, G.V., *Solid State Ionics*, 2001, vol. 145, pp. 205–210.
89. Lavrova, G.V., Russkikh, M.V., Ponomareva, V.G., and Uvarov, N.F., *Elektrokhimiya*, 2005, vol. 41, pp. 556–569.
90. Ponomareva, V.G., Lavrova, G.V., and Burgina, E.B., *Elektrokhimiya*, 2005, vol. 41, pp. 640–645.
91. Ponomareva, V.G., Lavrova, G.V., and Burgina, E.B., *Solid State Ionics*, 2005, vol. 176, pp. 767–771.
92. Leonova, L.S., Dobrovol'skii, Yu.A., Domashnev, D.I., Ukshe, A.E., Grebtsova, O.M., and Arkhangel'skii, I.V., *Elektrokhimiya*, 2003, vol. 39, pp. 552–558.
93. Diosa, J.E., Solis, A., Vargas, R.A., and Mellander, B.-E., *Solid State Ionics*, 2004, vol. 175, pp. 459–461.
94. Muroyama, H., Matsui, T., Kikuchi, R., and Eguchi, K., *J. Electrochem. Soc.*, 2006, vol. 153, pp. A1077–A1080.
95. Ponomareva, V.G., Tarnopolsky, V.A., Burgina, E.B., and Yaroslavl'tsev, A.B., *Mendeleev Commun.*, 2002, pp. 223–224.
96. Voropaeva, E.Yu., Stenina, I.A., and Yaroslavl'tsev, A.B., *Zh. Neorg. Khim.*, 2007, vol. 52, pp. 5–11.
97. Otomo, J., Minagawa, N., Wen, C.J., Eguchi, K., and Takahashi, H., *Solid State Ionics*, 2003, vol. 156, pp. 357–361.
98. Ponomareva, V.G., Shutova, E.S., and Matvienko, A.A., *Neorg. Mater.*, 2004, vol. 40, pp. 721–728.
99. Ponomareva, V.G. and Shutova, E.S., *Solid State Ionics*, 2005, vol. 176, pp. 2905–2908.
100. Ponomareva, V.G., Tarnopol'skii, V.A., and Yaroslavl'tsev, A.B., *Zh. Neorg. Khim.*, 2006, vol. 51, pp. 389–392.
101. Tarnopol'skii, V.A. and Yaroslavl'tsev, A.B., *Dokl. Ross. Akad. Nauk*, 2000, vol. 375, pp. 64–67.
102. Yaroslavl'tsev, A.B., *Defect Diffus. Forum*, 2003, vols. 216–217, pp. 133–141.
103. Sata, N., Ebermann, K., Eberl, K., and Maier, J., *Nature*, 2000, vol. 408, pp. 946–949.
104. Jin-Phillipp, N.Y., Sata, N., Maier, J., Scheu, C., Hahn, K., Kelsch, M., and Ruhlle, M., *J. Chem. Phys.*, 2004, vol. 120, pp. 2375–2381.
105. Nagai, M. and Nishino, T., *Solid State Ionics*, 1992, vols. 53–56, pp. 63–67.
106. Maekawa, H., Tanaka, R., Sato, Y., Fujimaki, Y., and Yamamura, T., *Solid State Ionics*, 2004, vol. 175, pp. 281–285.
107. Yaroslavl'tsev, A.B., Nikonenko, V.V., and Zabolotskii, V.I., *Usp. Khim.*, 2003, vol. 72, pp. 438–470.
108. Hsu, W.Y. and Gierke, T.D., *J. Membr. Sci.*, 1983, vol. 13, pp. 307–326.
109. Hsu, W.Y. and Gierke, T.D., *J. Electrochem. Soc.*, 1982, vol. 129, pp. C121–C121.
110. Gierke, T.D., Munn, G.E., and Wilson, F.C., *J. Polym. Sci. Polym. Phys. Ed.*, 1981, vol. 19, pp. 1687–1695.
111. Zabolotskii, V.I. and Nikonenko, V.V., *Perenos ionov v membranakh* (Ion Transport in Membranes), Moscow: Nauka, 1996.
112. Jones, L., Pintauro, P.N., and Tang, H.J., *Membr. Sci.*, 1999, vol. 162, pp. 135–143.
113. Trunov, V.A., Lebedev, V.T., Grushko, Yu.S., et al., *Kristallografiya*, 2007, vol. 52, pp. 536–539.
114. Chibirova, F.Kh., Zakhar'in, D.S., Timashev, S.F., Popkov, Yu.M., Sedov, V.E., Kornilova, A.A., and Reiman, S.I., *Zh. Fiz. Khim.*, 1988, vol. 62, pp. 645–651.
115. Volkov, I., Popkov, Yu.M., Timashev, S.F., Bes-sarabov, D.G., Sanderson, R.D., and Twardowski, Z., *J. Membr. Sci.*, 2000, vol. 180, pp. 1–13.
116. Berezina, N.P., Kononenko, N.A., and Vol'fkovich, Yu.M., *Elektrokhimiya*, 1994, vol. 30, pp. 366–372.
117. Masselin, I., Durand-Bourlier, L., Laine, J.-M., Sizaret, P.-Y., Chasseray, X., and Lemordant, D., *J. Membr. Sci.*, 2001, vol. 186, pp. 85–96.
118. Zabolotskii, V.I., Nikonenko, V.V., Kostenko, O.N., and El'nikova, L.F., *Zh. Fiz. Khim.*, 1993, vol. 67, pp. 2423–2427.
119. Jones, D.J. and Roziere, J., in *Handbook of Fuel Cells. Fundamentals, Technology, and Applications*, Vielstich, W., Gasteiger, H.A., and Lamm, A., Eds., vol. 3. *Fuel Cell Technology and Applications*, Wiley, 2003, pp. 447–455.
120. Yaroslavl'tsev, A.B., *Solid State Ionics*, 2005, vol. 176, pp. 2935–2940.
121. Peled, E., Duvdevani, T., and Milman, A., *Electrochem. Solid State Chem.*, 1998, vol. 1, pp. 210–211.
122. Baradie, B., Poinson, C., Sanchez, J.Y., Piffard, Y., Vitter, G., Bestaoui, N., Foscallo, D., Denoyelle, A., Delaouglise, D., and Vaujany, M., *J. Power Sour.*, 1998, vol. 74, pp. 8–16.
123. Bonnet, B., Jones, D.J., Roziere, J., Tchicaya, L., Alberti, G., Casciola, M., Massinelli, L., Bauer, B., Peraio, A., and Ramunni, E., *J. New Mater. Electrochem. Syst.*, 2000, vol. 3, pp. 87–92.
124. Staiti P., Minutoli, M., and Hocevar, S., *J. Power Sour.*, 2000, vol. 90, pp. 231–236.
125. Antonucci, P.L., Arico, A.S., Creti, P., Ramunni, E., and Antonucci, V., *Solid State Ionics*, 1999, vol. 125, pp. 431–437.

126. Amarilla, J.M., Rojas, R.M., Rojo, J.M., Cubillo, M.J., Linares, A., and Acosta, J.L., *Solid State Ionics*, 2000, vol. 127, pp. 133–139.
127. Di Noto, V., Gliubizzi, R., Negro, E., Vittadello, M., and Pace, G., *Electrochim. Acta*, 2007, vol. 53, pp. 1618–1627.
128. Matos, B.R., Santiago, E.I., Fonseca, F.C., Linardi, M., Lavayen, V., Lacerda, R.G., Ladeira, L.O., and Ferlauto, A.S., *J. Electrochem. Soc.*, 2007, vol. 154, pp. B1358–B1361.
129. Wu, Z., Sun, G., Jin, W., Hou, H., Wang, S., and Xin, Q., *J. Membr. Sci.*, 2008, vol. 313, pp. 336–343.
130. Park, K.T., Jung, U.H., Choi, D.W., Chun, K., Lee, H.M., and Kim, S.H., *J. Power Sour.*, 2008, vol. 177, pp. 247–253.
131. Tricoli, V. and Nannetti, F., *Electrochim. Acta*, 2003, vol. 48, pp. 2625–2633.
132. Song, M.-K., Park, S.-B., Kim, Y.-T., Rhee, H.-W., and Kim, J., *Mol. Cryst. Liq. Cryst.*, 2003, vol. 407, pp. 411–419.
133. Zaidi, S.M.J., Mikhailenko, S.D., Robertson, G.P., Guiver, M.D., and Kaliaguine, S., *J. Membr. Sci.*, 2000, vol. 173, pp. 17–34.
134. Tazi, B. and Savadogo, O., *Electrochim. Acta*, 2000, vol. 45, pp. 4329–4339.
135. Tazi, B. and Savadogo, O., *J. New Mater. Electrochem. Syst.*, 2001, vol. 4, pp. 187–196.
136. Ramani, V., Kunz, H.R., and Fenton, J.M., *J. Membr. Sci.*, 2004, vol. 232, pp. 31–44.
137. Xu, H., Wu, M., Liu, Y., Mittal, V., Vieth, R., Kunz, H.R., Bonville, L.J., and Fenton, J.M., *ECS Trans.*, 2006, vol. 3, pp. 561–568.
138. Costamagna, P., Yang, C., Bocarsly, A. B., and Srinivasan, S., *Electrochim. Acta*, 2002, vol. 47, pp. 1023–1033.
139. Yang, C., Srinivasan, S., Bocarsly, A.B., Tulyani, S., and Benziger, J.B., *J. Membr. Sci.*, 2004, vol. 237, pp. 145–161.
140. Alberti, G., Casciola, M., Capitani, D., Donnadio, A., Narducci, R., Pica, M., and Sganappa, M., *Electrochim. Acta*, 2007, vol. 52, pp. 8125–8132.
141. Tripathi, B.P. and Shahi, V.K., *J. Colloid Interface Sci.*, 2007, vol. 316, pp. 612–621.
142. Chen, L.-C., Yu, T.L., Lin, H.-L., and Yeh, S.-H., *J. Membr. Sci.*, 2008, vol. 307, pp. 10–20.
143. Deng, Q., Cable, K.M., Moore, R.B., and Mauritz, K.A., *J. Polym. Sci. B. Polym. Phys.*, 1996, vol. 34, pp. 1917–1923.
144. Voropaeva, E.Yu., Stenina, I.A., Yurkov, G.Yu., and Yaroslavl'tsev, A.B., *Zh. Neorg. Khim.*, 2008, vol. 53, pp. 1637–1642.
145. Baradie, B., Dodelet, J.P., and Guay, D., *J. Electroanal. Chem.*, 2000, vol. 489, pp. 101–105.
146. Novikova, S.A., Volodina, E.I., Pis'menskaya, N.D., Veresov, A.G., Stenina, I.A., and Yaroslavl'tsev, A.B., *Elektrokhimiya*, 2005, vol. 41, pp. 1203–1209.
147. Shalimov, A.S., Novikova, S.A., Stenina, I.A., and Yaroslavl'tsev, A.B., *Zh. Neorg. Khim.*, 2006, vol. 51, no. 5, pp. 767–772.
148. Fomenko, A.I., Pinus, I.Yu., Peregudov, A.S., Zubavichus, Ya.V., Khokhlov, A.R., and Yaroslavl'tsev, A.B., *Vysolomol. Soedin., Ser. A*, 2007, vol. 49, pp. 1299–1305.
149. Voropaeva, E.Yu., Stenina, I.A., and Yaroslavl'tsev, A.B., *Zh. Neorg. Khim.*, 2008, vol. 53, pp. 1797–1801.
150. Ponomarev, A.N., Moskvina, Yu.L., and Babenko, S.D., *Elektrokhimiya*, 2007, vol. 43, pp. 290–295.
151. Stenina, I.A., Il'ina, A.A., Pinus, I.Yu., Sergeev, V.G., and Yaroslavl'tsev, A.B., *Izv. Ross. Akad. Nauk, Ser. Khim.*, 2007, no. 11, pp. 2217–2220.
152. Berezina, N.P., Kubaisy, A.A.-R., Alpatova, N.M., Andreev, V.N., and Griga, E.I., *Elektrokhimiya*, 2004, vol. 40, pp. 333–341.
153. Berezina, N.P. and Kubaisy, A.A.-R., *Elektrokhimiya*, 2006, vol. 42, no. 1, pp. 91–99.
154. Berezina, N.P., Kubaisy, A.A.-R., Timofeev, S.V., and Karpenko, L.V., *J. Solid State Electrochem.*, 2006, vol. 11, pp. 378–389.
155. Barthet, C. and Guglielmi, M., *Electrochim. Acta*, 1996, vol. 41, pp. 2791–2798.
156. Shimizu, T., Naruhashi, T., Momma, T., and Osaka, T., *Electrochem. (Jpn.)*, 2002, vol. 70, pp. 991–993.
157. Chen, Y.-H., Wu, J.-Y., and Chung, Y.-C., *Biosens. Bioelectron.*, 2006, vol. 22, pp. 489–494.
158. Nagarale, R.K., Gohil, G.S., and Shahi, V.K., *J. Membr. Sci.*, 2006, vol. 280, pp. 389–396.